Top reduced cross section behavior at the LHeC kinematic range

G.R.Boroun*

Physics Department, Razi University, Kermanshah 67149, Iran
(Dated: July 27, 2016)

The linear and non-linear behavior of the top reduced cross section in the LHeC region is considered concerning the boson-gluon fusion (BGF) model at the deep inelastic scattering leptoproduction. We will show that the nonlinear behavior ,at this region, for the $t\bar{t}$ production is very small. Also the behavior of the top reduced cross section and the ratio R^t in this processes is considered.

arXiv:1510.02914v4 [hep-ph] 26 Jul 2016

1.Introduction

Recently there have been important researches on the $t\bar{t}$ production at the the Large Hadron Electron Collider (LHeC) project at CERN [1-3]. The LHeC shows an increase in the kinematic range of the deep inelastic scattering (DIS) and also an increase in the luminosity since this value is approximately $\simeq$ 100 fb^{-1}. As to exceed, the integrated HERA luminosity is realized by two orders of magnitude. This continues the path of deep inelastic scattering is the best tool to probe proton structure into unknown areas of physics and DIS kinematics. The DIS kinematics are $2 < Q^2 < 100,000\, GeV^2$ and $0.000002 < x < 0.8$ with a center-of-mass energy of about $\sqrt{s_{ep}} > 1\ TeV$ in accordance with the B scenario, as the kinematic range of the LHeC is illustrated in Fig.1. Clearly this increase in the precision of parton distribution functions (PDF·s) and in the low x kinematic region is realized by this project. As the strong rise of the reduced cross section is expected to appear due to the non-linear gluon-gluon interaction effects in the so-called saturation region.

In the neutral current deep inelastic scattering (NC DIS), the inclusive top electroproduction is dominantly by the boson-gluon fusion at $x \leq 0.1$ (Fig.2). The top flavor production has not been explored in NC DIS yet, because the cross section is too small ($\simeq 0.023pb$). In the Standard Model, a precise measurement of $t\bar{t}$ production in NC DIS is sensitive to the gluon distribution behavior [2], although the increase of the gluon density towards low x values must be tamed by the unitarity reasons (especially at "hot" spots in the proton).

In the framework of DGLAP dynamics [4-5], considering the heavy-flavor physics allowed a great advancement in understanding of the heavy quark production dynamics. New measurements of charm and beauty production at LHeC provide high precision pQCD tests as the LHeC is the ideal machine for a further extension on top production. As to the measurements of LHeC, the events with charm and beauty quarks increase of nearly $\sim$ %36 and $\sim$ %9 fraction of the total respectively, when compared with HERA data available. Due to the large gluon density at low x, the $t\bar{t}$ pair production dominantly via the direct BGF (Fig.2). In the high Q^2 limit, considering the top flavor physics is in the framework of fixed-flavor-number scheme (FFNS) [6-7] with $n_f = 5$. In general the measurement of the top structure function $F_2^{t\bar{t}}$ is the highest interest for theoretical analysis top quark in the final state. At sufficiently high $Q^2 >> m_t^2$ the top structure function can be directly related to effective densities of top quark in the proton.

The main purpose of this paper is the top reduced cross section behavior in the LHeC regions. Top reduced cross section will be presented in Sec.2. The nonlinear behavior is derived in Sec.3. Sec.4 contains the conclusions and discussions.

2.Top reduced cross section

We discuss the heavy flavor structure function $F_2(x, Q^2, m_H^2)$, that is sensitive to the shape of the gluon density at low x. The reaction under study is $e(p_e) + P(p) \rightarrow e(p'_e) + H(p_1)\overline{H}(p_1) + X$, where $H\overline{H}$ are heavy quark-antiquark pairs, such as $c\bar{c}, b\bar{b}$ or $t\bar{t}$, with momentum p_1 ($p_1{}^2 = m_H^2$) and X is any hadronic state allowed. These pair productions are dependent to the momentum carried by gluon distribution at low x. In the following, we are interesting to determine the reduced cross section of the top pair production in the LHeC region (Fig.1), although this cross section in NC DIS is small [3]. The top reduced cross section is given by the following form

$$\widetilde{\sigma}^t(x, Q^2, m_t^2) = F_2^t(x, Q^2, m_t^2)[1 - \frac{y^2}{1 + (1-y)^2} R^t], \quad (1)$$

where $R^t = \frac{F_L^t}{F_2^t}$. The inclusive top structure functions (F_2^t and F_L^t) at the leading order (LO) up to the next-to-leading order (NLO) analysis are given in Ref. [8] (where only the gluon distributions are considerable). The top

*Electronic address: grboroun@gmail.com; boroun@razi.ac.ir

structure functions are given by the following forms

$$F_k^t(x,Q^2,m_t^2)\simeq\frac{Q^2\alpha_s}{4\pi^2 m_t^2}\int_x^{z_{max}}\frac{dz}{z}[e_t^2 g(\frac{x}{z},\mu_t^2)C_{k,g}^{(0)t}$$
$$+\frac{Q^2\alpha_s^2}{\pi m_t^2}\int_x^{z_{max}}\frac{dz}{z}[e_t^2 g(\frac{x}{z},\mu_t^2)(C_{k,g}^{(1)t}+\overline{C}_{k,g}^{(1)t}\ln\frac{\mu_t^2}{m_t^2}), \quad (2)$$

where $k=2,L$ and the upper boundary on the integration is given by $z_{max}=\frac{Q^2}{Q^2+4m_t^2}$, with $m_t=175\ GeV$. One can consider the boundary condition according to the LHeC region, such that $z_{max}\to 0.9$ when $Q^2>4m_t^2$, $z_{max}\to 0.5$ when $Q^2=4m_t^2$ and $z_{max}\to 0$ when $Q^2<4m_t^2$. Here $g(x,\mu_t^2)$ is the gluon density and the scale $\mu_t(=\sqrt{\frac{Q^2}{2}+4m_t^2})$ is the mass factorization and the renormalization scale. The $\overline{MS}$ gluonic coefficient functions, $\{C_{k,g}^{(i)t}(\eta,\xi),\overline{C}_{k,g}^{(i)t}(\eta,\xi),i=0,1\}$, originate from those gluonic subprocesses where the virtual photon is coupled to the top pair quark via the boson-gluon fusion and they are dependent to the scaling variables $\eta\to\frac{s}{4m_t^2}$ and $\xi=\frac{Q^2}{m_t^2}$.

The top reduced cross section has been defined in Ref.[2]. Now, let us introduce the compact formula for the ratio R^t such that

$$R^t=\frac{C_{L,g}^{(i)t}(x,\xi)\otimes g(x,\mu_t^2)}{C_{2,g}^{(i)t}(x,\xi)\otimes g(x,\mu_t^2)}, \quad (3)$$

here symbol $\otimes$ is correspondent to the convolution over the variable x as: $a\otimes b[x]=\int_x^1\frac{dz}{z}a(z)b(\frac{x}{z})$. The ratio R^t, in top-quark leptoproduction, is a probe of the top content of the proton which greatly simplifies the extraction of F_2^t from measurements of the top reduced cross sections at the LHeC. Fig.3 shows the quantities R^c,R^b and R^t as a function of Q^2 for $x\leq 0.01$. The ratios R^c and R^b have approximately the same behavior and they are difference from the ratio R^t as these quantities are dependent to the gluon momentum, such that $x_g^t>x_g^b>x_g^c$ (in accordance with the heavy quark mass). These ratio·s are approximately independent of x at low x values. In Table 1, we see that $R^{max}\simeq 0.21$ for heavy quarks in a wide region of Q^2. We observe that the R^{max} predictions occurred in the region $Q^2>4m_H^2$, as the ratio·s $\frac{Q^2}{4m_H^2}$ are $11.11, 8.98$ and 8722.46 for production charm, beauty and top quarks respectively. One can consider the coefficient of R^t on a wide scale of the inelasticity y, such that $\frac{y^2}{1+(1-y)^2}\to 1$ at the LHeC region (Fig.1) and according to the center of mass energy. Thus the top reduced cross section can be rearranged by

$$\widetilde{\sigma}^t(x,Q^2,m_t^2)=F_2^t(x,Q^2,m_t^2)[1-R^t]. \quad (4)$$

At $Q^2\geq m_t^2$, the top structure function can be evaluated from the top reduced cross section according to Eq.4 as $F_2^t(x,Q^2,m_t^2)=\widetilde{\sigma}^t(x,Q^2,m_t^2)/[1-R^t]$ which implies that the R^t values are given by Eq.3. The gluon distribution to the top structure function is taken from MMHT14[10], NNPDF3[11] and CT14[12] at large scale μ_t^2. In what follows we need an analytical form for the gluon distribution. So we shall use the BDHM analysis [13] which extrapolated to the very low x values and high Q^2 values. The results (F_2^t and $\widetilde{\sigma}^t$) of our analysis at $Q^2\geq m_t^2$, on the top electroproduction, are collected in Fig.4. One can see that contribution of the top longitudinal structure function F_L^t to the top reduced cross section will be measurable in the LHeC kinematic range. For $Q^2<m_t^2$, the ratio R^t is very small. So with a good accuracy we will have

$$\widetilde{\sigma}^t(x,Q^2,m_t^2)\simeq F_2^t(x,Q^2,m_t^2). \quad (5)$$

At low x, where only the gluon contributions are considerable, the top contribution F_2^t to the proton structure function is given by this form

$$F_2^t(x,Q^2,m_t^2) = 2e_t^2\frac{\alpha_s(\mu_t^2)}{2\pi}\int_{1-\frac{1}{a}}^{1-x}dzC_{2,g}^{(i)t}(1-z,\frac{Q^2}{\mu_t^2})$$
$$\times G(\frac{x}{1-z},\mu_t^2), \quad (6)$$

where $a=1+4\frac{m_t^2}{Q^2}$, $G=xg$ is the gluon distribution function and $C_{2,g}^{(i)t}$·s are the top coefficient functions at LO and NLO analysis. In what follows it is convenient to use directly the gluon distribution behavior according to the Eq.6 as the top reduced cross section (Eq.5) modified by

$$\widetilde{\sigma}^t(x,Q^2,m_t^2)\propto C_{2,g}^{(i)t}(a_s,x,\frac{Q^2}{\mu_t^2})\otimes G(x,\mu_t^2). \quad (7)$$

This equation is valid when we will apply the high gluon density in accordance with the LHeC region at low x values. It provides a transition from the dilute side by decreasing x or by increasing the number of gluons in the proton. We will study this transition from the linear QCD evolution equations into the non-linear equations in the next section.

3.Nonlinearity

Within the standard framework of leading-twist linear QCD evolution equations (DGLAP), the gluon densities are predicted to rise at low x which is perceived in DIS experiments at HERA. At the LHeC low x domains we have expected that the growth of the top reduced cross section, with respect to the gluon densities, saturates by unitarity bound (caused by Froissart and Martin bounds [14]). This increase at low x should eventually be tames by the nonlinear effects of gluon density and it occurs when

chances of two gluons recombining into one and ,therefore, gluon recombination will be important concerning the gluon splitting. This nonlinear evolution leads to the phenomenon of saturation of gluonic density in the nucleon which can be exploited to the DIS of the LHeC at the high centre-of-mass energy(i.e. extending the kinematic range to lower x).
This recombination leads to the modification of the linear DGLAP evolution equation by a term which is nonlinear in gluon density. The first equation of this type reporting the fusion of two gluon ladders into on. This picture allows us to write the Gribov- Levin -Ryskin-Mueller- Qiu (GLR-MQ) [15-16] equation for the gluon distribution at low x. In double leading logarithmic approximation (DLLA, $\ln 1/x \ln Q^2 >> 1$), GLR-MQ have been determined a new nonlinear evolution equation for gluon density because the negative sign in front of the nonlinear term responsible to the gluon recombination, as:

$$Q^2\frac{\partial^2 G(x,Q^2)}{\partial \ln\frac{1}{x}\partial Q^2} = \frac{\alpha_s N_c}{\pi}G(x,Q^2) - \frac{4\alpha_s^2 N_c}{3C_F R^2}\frac{1}{Q^2}[G(x,Q^2)]^2, \quad (8)$$

in which the parameter R control the strength of the nonlinearity and it is the correlation radius between two interaction gluons when that gluons are concentrated in hot- spot [17] point ($R \simeq 2\ GeV^{-1}$) within the proton.
Thus the Q^2 evaluation of the gluon distribution function (Eq.8) with nonlinear effects, can be rewritten as

$$\frac{\partial G(x,Q^2)}{\partial \ln Q^2} = \frac{\partial G(x,Q^2)}{\partial \ln Q^2}|_{DGLAP} - \frac{81\alpha_s^2}{16R^2Q^2}\int_\chi^1 \frac{dy}{y}[G(y,Q^2)]^2, \quad (9)$$

where $\chi = \frac{x}{x_0}$ and $x_0 = 0.01$ is the boundary condition between the shadowing and unshadowing region that the gluon distribution joints smoothly onto the unshadowed region ($x > x_0$). The first term in the r.h.s of Eq.9 is the standard linear DGLAP evolution that can be expressed at low x as

$$\frac{\partial G(x,Q^2)}{\partial \ln Q^2}|_{DGLAP} \simeq \frac{\alpha_s}{2\pi}[P_{gg}(x,\alpha_s)\otimes G(x,Q^2)], \quad (10)$$

here the splitting function P_{gg} can be ordered in running coupling constant $\alpha_s(Q^2)$. The second term in the r.h.s of Eq.9 is the nonlinear shadowing term. This shadowing effects, arises from the two gluon ladders recombine into a single one. Therefore the gluon distribution function modified by the following form [18-19]

$$\frac{\partial G(x,Q^2)}{\partial \ln Q^2} = \frac{\alpha_s}{2\pi}P_{gg}(x,\alpha_s)\otimes G(x,Q^2) - \frac{81\alpha_s^2}{16R^2Q^2}\int_\chi^1 \frac{dy}{y}[G(y,Q^2)]^2. \quad (11)$$

The solution of Eq.11 is straightforward and given by

$$G(x,Q^2) = \frac{M(x,Q^2)}{C - N(x,Q^2)\Gamma[-1+M(x),Q^2]}, \quad (12)$$

in which the functions of M and N are dependent on the coefficients of $G(x,Q^2)$ and $G^2(x,Q^2)$ in the r.h.s of Eq.11 respectively, also Γ is the incomplete gamma function and C is dependent to the initial condition of the gluon distribution at $Q^2 = Q_0^2$. The shadowing correction to the gluon distribution at the initial scale defined by $G(x,Q_0^2)$. As, the low x behavior of the shadowing corrections to the gluon distribution at Q_0^2 is assumed to be [20]

$$G(x,Q_0^2) = G^u(x,Q_0^2)[1+\theta(x_0-x)[G^u(x,Q_0^2) - G^u(x_0,Q_0^2)]/G^{sat}(x,Q_0^2)]^{-1}, \quad (13)$$

where $G^{sat}(x,Q^2) = \frac{16R^2Q^2}{27\pi\alpha_s(Q^2)}$ is the value of the gluon which would saturate the unitarity limit in the leading shadowing approximation and $G^u(x,Q_0^2)$ that is the input unshadowing gluon distribution taken from the QCD parametrisation.
Now, we have the shadowing correction to the initial gluon distribution, then inserting Eq.13 in Eq.12, therefore the C constant in Eq.12 is dependence upon the initial condition as it follows:

$$G(x,Q^2) = \frac{M(x,Q^2)G^u(x,Q_0^2)}{M(x,Q_0^2)[1+\frac{\theta(x_0-x)[G^u(x,Q_0^2)-G^u(x_0,Q_0^2)]}{G^{sat}(x,Q_0^2)}] + \{N(x,Q_0^2)\Gamma[-1+M(x),Q_0^2] - N(x,Q^2)\Gamma[-1+M(x),Q^2]\}G^u(x,Q_0^2)}. \quad (14)$$

Therefore the shadowing correction to the top reduced cross section is corespondent to the nonlinear gluon distribution function at scale μ_t^2 by the following form:

$$\widetilde{\sigma}^t(x,Q^2,m_t^2) \simeq \; 2e_t^2\frac{\alpha_s(\mu_t^2)}{2\pi}C_{2,g}^{(i)t}(a_s,x,\frac{Q^2}{\mu_t^2})\otimes \frac{M(x,\mu_t^2)G^u(x,\mu_{0t}^2)}{M(x,\mu_{0t}^2)[1+\frac{\theta(x_0-x)[G^u(x,\mu_{0t}^2)-G^u(x_0,\mu_{0t}^2)]}{G^{sat}(x,\mu_{0t}^2)}]+\{N(x,\mu_{0t}^2)\Gamma[-1+M(x),\mu_{0t}^2]-N(x,\mu_t^2)\Gamma[-1+M(x),\mu_t^2]\}G^u(x,\mu_{0t}^2)}. \quad (15)$$

This equation shows that the top reduced cross section behavior is tamed due to the saturation effects at low x. At the LHeC region for $Q^2 < 1000\ GeV^2$ we observed that $\mu_t^2 \simeq 4m_t^2$, therefore the coefficient of the nonlinear term (second term in the r.h.s of Eq.9) is very very small and the shadowing correction to the top reduced cross section is not worthwhile. We believe that this behavior for the nonlinear term at low Q^2 values is correct, because within the color dipole approach [21] the $t\overline{t}$ color dipole size is very small than the charm and bottom size ($0.037 \leq r_c \leq 0.130fm$ and $0.014 \leq r_b \leq 0.043fm$) as

$$\frac{4}{Q^2+4m_t^2} \leq r_t^2 \leq \frac{1}{m_t^2} \Rightarrow r_t \simeq \; 0.0013\ fm. \quad (16)$$

We observe that the minimum and maximum distances, related to the $t\overline{t}$ interaction in the color dipole model, are the same one value $0.0013\ fm$. The color dipole size shows the sticking of the $t\overline{t}$ pair production, therefore in this case the nonlinear effects can be neglected for the LHeC region. So we can conclude that the shadowing corrections to the top reduced cross sections are very small in accordance with the LHeC region. On the other hand, in the region of low- x and Q^2 values, the process of gluon recombination does not play an important role on the $t\overline{t}$ production and therefore the nonlinear corrections to the top reduced cross section is not essential at this region. In Fig.5 we show our results for $Q^2 = 100\ GeV^2$, as the top reduced cross sections are very small for measurements.

4.Conclusion

We have obtained the ratio $R^t = F_2^t/F_L^t$ at the LHeC regions for the top pair production. We demonstrated the relation between the top reduced cross section and the top structure function by this ratio (R^t) at $Q^2 \geq m_t^2$ and $Q^2 < m_t^2$ regions. The linear and nonlinear behaviors considered and shows that the nonlinear behavior has a very small content for prob at very low x in which the gluon saturation is dominance.

Acknowledgments

Author is grateful to Prof.N.Armesto for suggestion, reading the manuscript and useful comments.

REFERENCES

1. LHeC workshops 2015 (http://cern.ch/lhec).
2.G.R.Boroun, Phys.Lett.B**744** (2015)142; Phys.Lett.B**741** (2015)197.
3. J.L.Abelleira Fernandez, et.al., [LHeC Collab.], J.Phys.G**39** (2012)075001.
4. V.N. Gribov and L.N. Lipatov, Sov. J. Nucl. Phys.**18** (1972) 438.
5. L.N. Lipatov, Sov. J. Nucl. Phys.**20** (1975) 93; G. Altarelli and G. Parisi, Nucl. Phys. B**126** (1977) 298; Yu.L. Dokshitzer, Sov. Phys. JETP **46** (1977) 641.
6. M.A.G.Aivazis, et.al., Phys.Rev.D**50** (1994) 3102.
7. J.C.Collins, Phys.Rev.D**58** (1998) 094002.
8.E. Laenen, S. Riemersma, J. Smith and W.L. van Neerven, Nucl. Phys. B**392** (1993) 162; S. Riemersma, J. Smith and W.L. van Neerven, Phys.Lett.B**347** (1995) 143.
9. A. Y. Illarionov,B. A. Kniehl and A. V. Kotikov, Phys.Lett. B **663** (2008)66.
10. L.A Harland-Lang, et.al., Eur.Phys.J.C**75** (2014) 435.
11. Richard D. Ball, et.al., NNPDF Collaboration, JHEP**04** (2015) 040.
12. S.Dulat, et.al., arXiv:1506.07443 [hep-ph] (2016).
13. Martin M.Block, et.al., Phys. Rev. D**88** (2013) 014006; Phys. Rev. D**88** (2013) 013003.
14. M. Froissart, Phys. Rev. **123** (1961) 1053; A. Martin, Phys. Rev. **129** (1963) 1432.
15. L.V.Gribov, E.M.Levin and M.G.Ryskin,

TABLE I: Maximum values of R^H extracted from Eq.3.

$Q^2(GeV^2)$	R^c_{max}	R^b_{max}	R^t_{max}
100	0.2106	—	—
750	—	0.2086	—
860000	—	—	0.2093

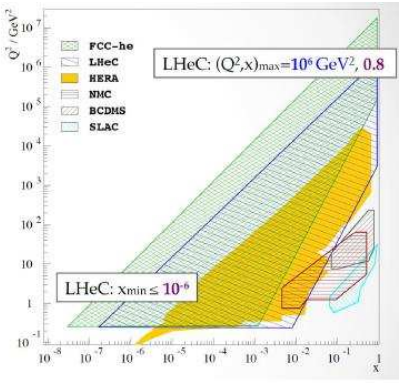

FIG. 1: Kinematic plane (Q^2, x) at the LHeC region.

Phys.Rep.**100** (1983)1.
16. A.H.Mueller and J.Qiu, Nucl.Phys.B**268** (1986)427.
17. E.M.Levin and M.G.Ryskin, Phys.Rep.**189** (1990)267.
18. G.R.Boroun, JETP**106**(2008)701; G.R.Boroun and B.Rezaei, Eur.Phys.J.C**73** (2013)2412.
19. G.R.Boroun, Eur.Phys.J.A**42** (2009)251; G.R. Boroun and S. Zarrin, Eur.Phys.J.Plus**128** (2013)119.
20. A.D. Martin, W.J. Stirling, R.G. Roberts, R.S. Thorne, Phys. Rev. D **47** (1993) 867; J. Kwiecinski, A.D. Martin, P.J. Sutton, Phys. Rev. D**44** (1991) 2640; A.J. Askew, J. Kwiecinski, A.D. Martin, P.J. Sutton, Phys. Rev. D**47** (1993) 3775.
21.R.Fiore, N.N.Nikolaev and V.R.Zoller, JETP Lett.**90** (2009)319.

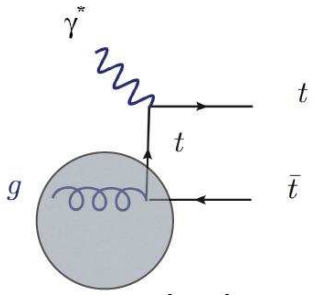

FIG. 2: Leading order Boson Gluon Fusion (BGF) diagram for $t\bar{t}$ production in ep-collisions.

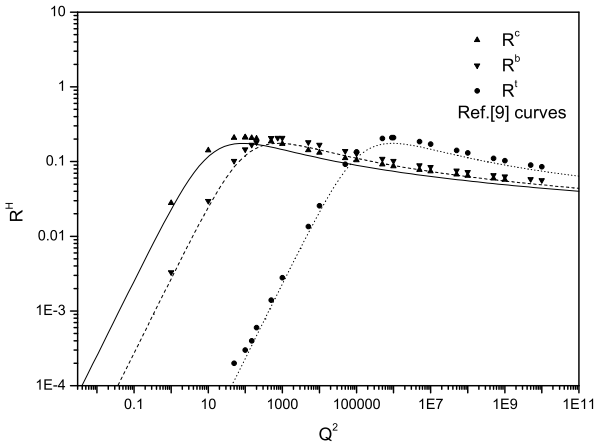

FIG. 3: R^H 's evaluated as functions of Q^2 at NLO analysis with $< \mu_H^2 >= 4m_H^2 + \frac{Q^2}{2}$, compared with curves estimated in Ref.[9].

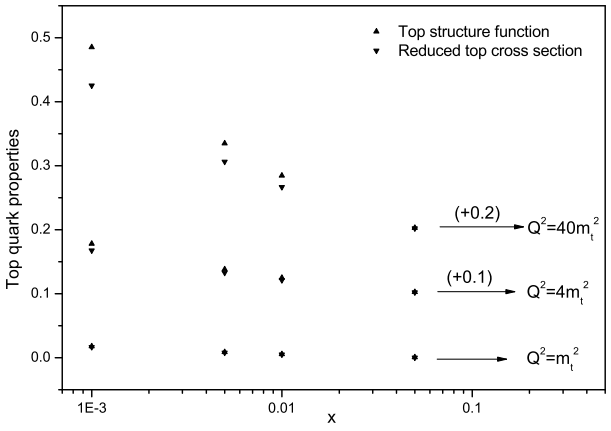

FIG. 4: Top structure function F_2^t and top reduced cross section $\widetilde{\sigma}^t$ determined from Eq.4 at $Q^2 = m_t^2, 4m_t^2$ and $40m_t^2$ GeV^2 according to the LHeC region.

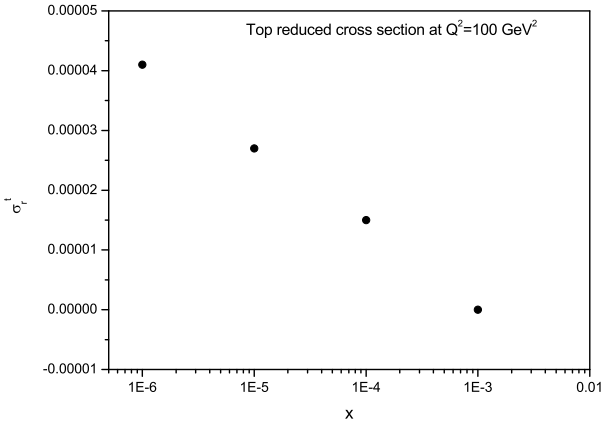

FIG. 5: Top reduced cross section $\widetilde{\sigma}^t$ determined from Eq.15 at $Q^2 = 100\ GeV^2$ according to the LHeC region.